Analysis of Round-Trip Efficiency of an HVAC-Based Virtual Battery

Naren Srivaths RAMAN^{1*}, Prabir BAROOAH¹

¹University of Florida, Department of Mechanical and Aerospace Engineering, Gainesville, Florida, USA Email: narensraman@ufl.edu, pbarooah@ufl.edu

*Corresponding Author

ABSTRACT

The flexibility in power consumption of heating, ventilation, and air-conditioning (HVAC) systems in buildings can be utilized to provide a battery-like service to the power grid. Recent work has reported that using HVAC systems in such a manner may lead to a net increase in energy consumption compared to normal operation, similar to a low round-trip efficiency (RTE) of a battery. In our previous work we showed that the low RTEs reported were due to the way the experiments/simulations were performed, and that using an HVAC system as a virtual battery repeatedly leads to an asymptotic RTE of one. In this work we show that when an additional constraint is imposed—that the mean temperature of the building must remain at its baseline value—the asymptotic RTE can be lower than one. We numerically investigate dependence on parameters such as building size and time period of charging/discharging.

1. INTRODUCTION

With increasing penetration of intermittent renewable energy sources, there is a growing recognition that the flexibility in demand of most electric loads can be utilized to provide ancillary services to the grid, such as frequency regulation (Lin et al., 2015; Makarov et al., 2008). In fact, loads can provide Virtual Energy Storage (VES) by varying their demand over a baseline so that to the grid they appear to be providing the same service as a battery (Cheng et al., 2017). Such a load, or collection of loads, can be called virtual batteries (VB).

The key constraint is to do so without violating consumers' quality of service (QoS). Two most important QoS measures for heating, ventilation, and air-conditioning (HVAC) systems are indoor temperature and total energy consumption. Experimental demonstration has shown that HVAC systems can provide VES service, especially in the fast time scale of "frequency regulation", with little or no discernible effect on the indoor temperature (Lin et al., 2015). Continuously varying the power consumption of loads around a baseline may lead to a net increase in the energy consumption when compared to nominal usage. If so, that will be analogous to the virtual battery having a round-trip efficiency (RTE) less than unity. Electrochemical batteries also have a less-than-unity round-trip efficiency (Luo et al., 2015), since not all the energy consumed during charging is returned to the grid during discharging.

In this paper we analyze the RTE of virtual battery comprised of HVAC equipment in commercial buildings. The inspiration for this paper comes from (Beil et al., 2015) and its follow-on works (Lin et al., 2017; Raman & Barooah, 2018). To the best of our knowledge, the article (Beil et al., 2015) is the first to provide experimental data on the RTE of commercial buildings providing VES. The experiments were conducted at a $\sim 30,000~m^2$ office building located in the Los Alamos National Laboratory (LANL) campus. In the experiments reported, the fan power was varied in an approximately square wave fashion with a time period of 30 minutes by changing in unison the thermostat set point of all the zones in the building. After one cycle of the square wave, the building was brought back to its baseline thermostat setpoint. It was observed that a considerable amount of additional energy had to be consumed to bring back the building to its baseline temperature in almost all the tests performed. This loss was expressed as a round-trip efficiency less than 1. The average RTE reported was less than 0.5. These values are low compared to that for Li-ion batteries, which vary from 0.75 to 0.97 (Luo et al., 2015). An RTE value much less than 1 indicates that use of HVAC systems as virtual batteries may not be cost effective.

The paper (Lin et al., 2017) investigated potential causes for the RTE values reported in (Beil et al., 2015) by conducting simulations. They also explored the effect of building parameters, control design, and imprecise knowledge

of baseline power consumption on the RTE. They were able to replicate several trends observed in the LANL experiments, but there were also significant differences.

In (Raman & Barooah, 2018), it was shown that the RTE values much smaller than unity that were reported in prior work were an artifact of the experimental/simulation set up. When the HVAC system is repeatedly used as a VES system the asymptotic RTE is one. The biggest difference between (Beil et al., 2015; Lin et al., 2017) and (Raman & Barooah, 2018) is that, the former considered only a single cycle of the square wave power variation while the latter considered multiple cycles. An important phenomenon that was observed in (Raman & Barooah, 2018) was that when the HVAC system's power consumption was repeatedly increased and decreased to act as a virtual battery, there was on average a slight warming of the building, (i.e., the average temperature deviation was above zero) even though the temperature deviation was within the user specified limits.

In this paper we examine on what happens to the asymptotic RTE, when the average temperature deviation from the baseline is constrained to be zero. Compared to (Raman & Barooah, 2018), this paper makes two contributions. First, we show that when the average steady state temperature of the building is constrained to be the same as the baseline value, an additional energy consumption may be needed which reduces the asymptotic RTE to strictly below 1. Second, we examine how this RTE varies with various parameters such as building size and time period of power deviation. The trends observed are valuable in choosing design parameters, such as whether a smaller or larger building is better suited to provide VES service.

2. DEFINITIONS AND OTHER PRELIMINARIES

For the sake of completeness we first present some of the definitions, mathematical models, and results from (Raman & Barooah, 2018). Consider an HVAC system whose power demand is artificially varied from its baseline demand to provide virtual energy storage. The power consumption of the virtual battery, \tilde{P} , is defined as the deviation of the electrical power consumption of the HVAC system from the baseline power consumption: $\tilde{P}(t) := P_{\text{HVAC}}(t) - P_{\text{HVAC}}^{(b)}(t)$, where $P_{\text{HVAC}}^{(b)}$ is the baseline power consumption of the HVAC system, defined as the power the HVAC system needs to consume to maintain a baseline indoor temperature $T^{(b)}$.

We now define the state of charge (SoC) of a virtual battery. Just as the SoC of a real battery must be kept between 0 and 1, the temperature of a building must be kept between a minimum value, denoted by T_L (low), and a maximum value, denoted by T_H (high), to ensure QoS. We therefore define the SoC of an HVAC-based virtual battery as follows.

Definition 1 (SoC of a VES system). (Raman & Barooah, 2018) The state of charge (SoC) of an HVAC-based VES system with indoor temperature T is the ratio $\frac{T_H - T}{T_H - T_L}$ where $[T_L, T_H]$ is the allowable range of indoor temperature.

Definition 2 (Complete charge-discharge). (Raman & Barooah, 2018) We say a virtual battery has undergone a complete charge-discharge during a time interval $[t_i, t_f]$ if $SoC(t_i) = SoC(t_f)$. The time interval $[t_i, t_f]$ is called a complete charge-discharge period.

The qualifier "complete" just means that the SoC comes back to where it started from, and has nothing to do with the SoC reaching 1 or 0.

Definition 3 (RTE). (Raman & Barooah, 2018) Suppose a virtual battery undergoes a complete charge-discharge over a time interval $[0, t_{cd}]$. Let t_c be the length of time during which the virtual battery is charging and t_d be the length of time during which the virtual battery is discharging so that $t_c + t_d = t_{cd}$. The round-trip efficiency (RTE) of the virtual battery, denoted by $\eta_{\rm RT}$, during this period is

$$\eta_{\rm RT} \triangleq \frac{E_d}{E_c} = \frac{-\int_{t_d} \tilde{P}(t)dt}{\int_{t_c} \tilde{P}(t)dt} = \frac{-\int_{t_d} (P_{\rm HVAC}(t) - P_{\rm HVAC}^{(b)}(t))dt}{\int_{t_c} (P_{\rm HVAC}(t) - P_{\rm HVAC}^{(b)}(t))dt}$$
(1)

where E_d is the energy released by the virtual battery to the grid during discharging, E_c is the energy consumed by the virtual battery from the grid during charging, and \int_{t_c} (resp., \int_{t_d}) denotes integration performed over the charging times (resp., discharging times).

3. MODEL OF AN HVAC-BASED VES SYSTEM

Figure 1 shows the schematic of a simplified variable-air-volume (VAV) HVAC system for a single zone under study. The only equipments that consume significant amount of electricity are the supply air fan and the chiller. We assume that the energy consumed by other equipments such as the chilled water pump motors is negligible. In the sequel, m_a denotes the air flow rate¹. Under baseline conditions, a climate control system determines the set point for the air flow rate, and the fan speed is varied to maintain that set point. The HVAC system is converted to a VES system with the help of an additional control system, which we denote by "VES controller". The VES controller modifies the set point of the air flow rate (that is otherwise decided by the climate control system) so that the power consumption of the virtual battery, $\tilde{P}(t)$, tracks an exogenous reference signal, $\tilde{P}^r(t)$. We assume that the VES controller is perfect; it can determine the variation in air flow required to track a power deviation reference exactly.

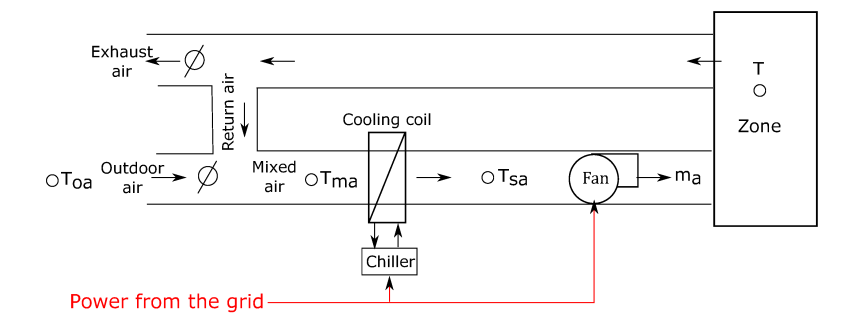


Figure 1: Simplified schematic of a commercial variable-air-volume HVAC system for a single zone.

3.1 Thermal Dynamics and HVAC Power Consumption Model

The following simple resistor-capacitor (RC) network model is used to model the temperature of the zone serviced by the HVAC system:

$$\dot{T} = \frac{1}{RC}(T_{oa} - T) + \frac{1}{C}q_x + \frac{1}{C}m_aC_{pa}(T_{sa} - T),\tag{2}$$

where R is the building structure's resistance to heat exchange between indoors and outdoors, C is the thermal capacitance of the building, T_{oa} is the outdoor air temperature, q_x is the exogenous heat influx into the building, T_{sa} is the supply air temperature, m_a is the mass flow rate of supply air, and C_{pa} is the specific heat capacity of dry air.

The power consumption of the HVAC system is a sum of the fan power and chiller power: $P_{\text{HVAC}}(t) = P_f(t) + P_{ch}(t)$. We model P_f as a quadratic in air flow rate and P_{ch} as being proportional to the heat it extracts from the mixed air stream that passes through the evaporator (or the cooling coil in a chilled water system). Therefore we get the following model:

$$P_{\text{HVAC}}(m_a, T) = \alpha_{1f}(m_a)^2 + \alpha_{2f}m_a + \frac{m_a C_{pa}[r_{oa}T_{oa} + (1 - r_{oa})T - T_{sa}]}{COP},$$
(3)

where α_{1f} and α_{2f} are coefficients that depend on the fan, COP is the coefficient of performance of the chiller, and r_{oa} is the ratio of outside air flow rate to total air flow rate, $r_{oa} := \frac{m_{oa}}{m_a}$.

We assume the following throughout the paper to simplify the analysis. (a) The ambient temperature (T_{oa}) , the exogenous heat gain (q_x) , and the coefficient of performance of the chiller (COP) are constants. (b) The ambient is warmer than the maximum allowable indoor temperature: $T_{oa} > T_H$, so the HVAC system only provides cooling. (c) Effect of humidity change is ignored. (d) The supply air temperature, T_{sa} , is constant, and $T_{sa} < T^{(b)}$.

¹Customarily air flow rate is denoted by \dot{m} . Since the notation \dot{x} is used for state derivatives (as in $\dot{x} = f(x, u)$), whereas air flow rate is an input (u) and not a state (x), we avoid the "dot" notation for air flow rate.

For a given baseline zone temperature $T^{(b)}$, T_{oa} , q_x , and T_{sa} the corresponding baseline air flow rate $m_a^{(b)}$ is given by:

$$0 = \frac{1}{R}(T_{oa} - T^{(b)}) + q_x + m_a^{(b)}C_{pa}(T_{sa} - T^{(b)}).$$
(4)

The baseline power consumption, $P_{\text{HVAC}}^{(b)}$, is obtained by plugging in $T^{(b)}$ and $m_a^{(b)}$ into the expression for P_{HVAC} in (3).

3.2 VES System Dynamics and Power Consumption

Let $\tilde{m}_a(t) := m_a(t) - m_a^{(b)}$, be the air flow rate deviation (from baseline) commanded by the VES controller. Let the resulting deviation in the zone temperature be:

$$\tilde{T}(t) := T(t) - T^{(b)}.$$
 (5)

The power consumed by the virtual battery is: $\tilde{P}(t) := P_{\text{HVAC}}(m_a(t), T(t)) - P_{\text{HVAC}}^{(b)}(m_a^{(b)}, T^{(b)})$, where $P_{\text{HVAC}}(\cdot, \cdot)$ is given by (3). By expanding the above equation for \tilde{P} , we obtain:

$$\tilde{P} = a\tilde{m}_a + b\tilde{T} + c\tilde{m}_a\tilde{T} + d\tilde{m}_a^2, \tag{6}$$

where
$$a := 2\alpha_{1f}m_a^{(b)} + \alpha_{2f} + \frac{C_{pa}[r_{oa}T_{oa} + (1 - r_{oa})T^{(b)} - T_{sa}]}{COP}$$
, (7)

$$b := \frac{C_{pa}m_a^{(b)}(1 - r_{oa})}{COP}, c := \frac{C_{pa}(1 - r_{oa})}{COP}, d := \alpha_{1f}.$$
 (8)

Differentiating (5), and using (2) and (4) we obtain:

$$\dot{\tilde{T}} = -\alpha \tilde{T} - \beta \tilde{m}_a - \gamma \tilde{T} \tilde{m}_a, \text{ where } \alpha := \frac{RC_{pa} m_a^{(b)} + 1}{RC}, \beta := \frac{C_{pa} (T^{(b)} - T_{sa})}{C}, \gamma := \frac{C_{pa}}{C}. \tag{9}$$

The dynamics of the temperature deviation (and therefore of the SoC of the virtual battery) are thus a differential algebraic equation (DAE): $\dot{\tilde{T}} = f(\tilde{T}, \tilde{m}_a)$, $\tilde{P} = g(\tilde{T}, \tilde{m}_a)$, where the first (differential) equation is given by (9) and the second (algebraic) equation is given by (6).

3.3 Numerical Computations

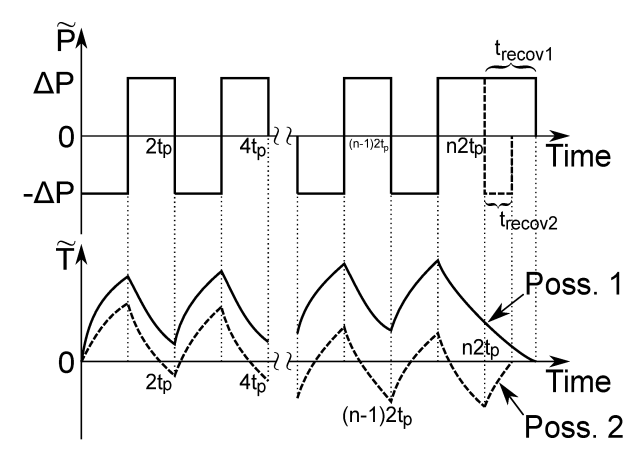
The parameters used for simulations are listed in Table 1. The values for R, C, $m_a^{(b)}$, α_{1f} , and α_{2f} are based on an auditorium ($\sim 6m$ high, floor area of $\sim 465m^2$) in Pugh Hall located in the University of Florida campus. The R and C values were chosen guided by (Lin, 2014). Using the values listed in Table 1 the baseline power consumption of the HVAC system turned out to be $P_{\rm HVAC}^{(b)} = 9725.6$ W. We used first-order Euler's method with time step of 0.1 seconds for simulations.

Parameter	Value	Parameter	Value	Parameter	Value
$T^{(b)}$	295.4 K	T_L	294.3 K	T_H	296.5 K
$m_a^{(b)}$	2.27 kg/s	C	$3.4 \times 10^{7} \text{ J/K}$	R	$1.3 \times 10^{-3} \text{ K/W}$
COP	3.5	α_{1f}	662 W/(kg/s) ²	α_{2f}	-576 W/(kg/s)
T_{sa}	285.9 K	T_{og}	299.8 K	-	

Table 1: Simulation parameters

4. RTE WITH ZERO-MEAN SQUARE-WAVE POWER CONSUMPTION

In this section we present some important results from (Raman & Barooah, 2018) for the sake of completeness. In order to enable comparison with prior works (Beil et al., 2015; Lin et al., 2017) we restrict the power consumption of the virtual battery to a square-wave signal. Since (Beil et al., 2015) reported differences in observed RTE depending on whether the power consumption is first increased and then decreased from the baseline ("up/down" cycle), or vice versa ("down/up" cycle), we also treat them separately.



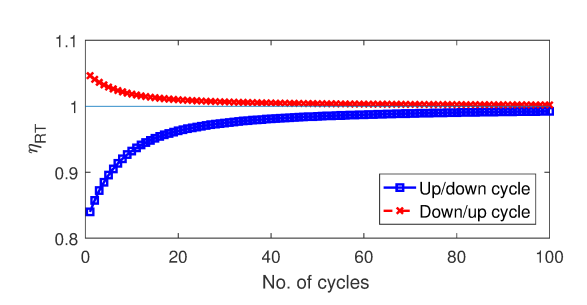


Figure 2: Additional charging or discharging needed to bring back \tilde{T} to its initial value (=0) after n periods of down/up cycle.

Figure 3: $\eta_{\rm RT}(n)$ vs. n, when the virtual battery tracks a square-wave power reference ($\Delta P=0.2P_{\rm HVAC}^{(b)}=1945.1~{\rm W}, r_{oa}=0.5,$ and $2t_p=3600$ seconds).

Let the amplitude of the power consumption $\tilde{P}(t)$ be ΔP and the time period be $2t_p$. For one half of the period, $\tilde{P}(t) = \Delta P$, and for the other half, $\tilde{P}(t) = -\Delta P$. Let us consider n periods of the square-wave power consumption signal, $n \geq 1$. At the end of n periods, the temperature deviation may not be exactly 0 (i.e., $\tilde{T}(n2t_p) \neq 0$), even though its initial value was 0 (i.e., $\tilde{T}(0) = 0$). Charging or discharging might be needed for an additional amount of time t_{recov} to bring the temperature deviation back to 0 (its initial value). Whether recovery to the initial \tilde{T} (and therefore the initial SoC of the virtual battery, see Definition 1) value requires additional charging or additional discharging depends on whether $\tilde{T}(n2t_p)$ is positive or negative. In either case, since $\tilde{T}(0) = \tilde{T}(n2t_p + t_{recov}) = 0$, according to Definition 2, the time interval $[0, n2t_p + t_{recov}]$ constitutes a complete charge-discharge period of the virtual battery. The RTE computed over this period using Definition 3 is called the RTE for n cycles or $\eta_{\rm RT}(n)$.

Figure 2 shows an illustration of the two possible scenarios for the possible values of $\tilde{T}(n2t_p)$. For the sake of concreteness, we have assumed the VES service starts with a down/up cycle in the figure. In the first possibility, denoted by the solid lines, $\tilde{T}(n2t_p) \geq 0$, and therefore additional charging is performed for $t_{recov1} \geq 0$ amount of time in order to bring the temperature deviation to 0. If this possibility were to occur, within the complete charge-discharge period $n2t_p + t_{recov1}$, the charging time is $nt_p + t_{recov1}$, while the discharging time is nt_p . It now follows from Definition 3 that for possibility 1,

$$\eta_{\text{RT}}(n) = \frac{-\int_{t_d} [-\Delta P] dt}{\int_{t_c} [\Delta P] dt} = \frac{t_d}{t_c} = \frac{nt_p}{nt_p + t_{recov1}(n)} \le 1.$$

$$(10)$$

In the second possibility, denoted by the dashed lines, $\tilde{T}(n2t_p) \leq 0$ and therefore additional discharging is needed for $t_{recov2} \geq 0$ amount of time. For this possibility,

$$\eta_{\text{RT}}(n) = \frac{-\int_{t_d} [-\Delta P] dt}{\int_{t_c} [\Delta P] dt} = \frac{t_d}{t_c} = \frac{nt_p + t_{recov2}(n)}{nt_p} \ge 1.$$
(11)

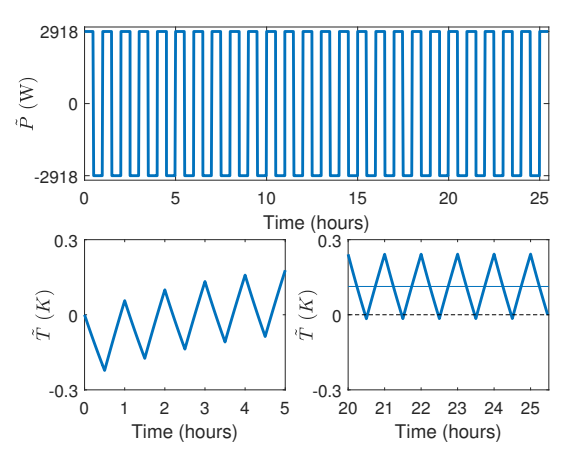
If the VES service were to start with an up/down cycle, the same two possibilities exist in principle, so again the RTE can be smaller or larger than one depending on whether the temperature deviation at the end of the n periods is positive or negative. It was shown in (Raman & Barooah, 2018) that the temperature deviation is bounded by a constant independent of n under the assumption that $\tilde{T}(0) = 0$. Therefore the recovery times in (10) and (11) will also be bounded. The following theorem says that the RTE tends to 1 as the number of cycles tends to infinity, irrespective of whether it starts with an up/down or down/up cycle.

Theorem 1. (Raman & Barooah, 2018) If $r_{oa} = 1$, $\lim_{n \to \infty} \eta_{RT}(n) = 1$.

For the proof of the above theorem and a detailed discussion, interested readers are referred to (Raman & Barooah, 2018). Figure 3 shows numerically computed values of $\eta_{RT}(n)$ as a function of n and verifies the prediction of Theorem 1.

5. RTE WITH NONZERO-MEAN SOUARE-WAVE POWER CONSUMPTION

In the previous section, the power deviation signal $\tilde{P}(t)$ was zero-mean. However, the resulting zone temperature deviation from baseline may not be zero-mean. One may argue that to perform a fair comparison, the mean temperature deviation at steady state must be kept at zero somehow. Such a change may necessitate additional power consumption, which may change the asymptotic RTE away from unity. Figure 4 shows numerical evidence of such a phenomenon: $\tilde{P}(t)$ is a zero-mean square wave with amplitude $\Delta P = 2917.7~{
m W}$ (30% of the baseline power consumption $P_{
m HVAC}^{(b)} =$ 9725.6 W). When the temperature deviation $\tilde{T}(t)$ reaches periodic steady state, its average value over one cycle is ~ 0.11 K. If ΔP were to be 20% and 40% of the baseline, the average temperature deviation turns out to be 0.05 K and 0.21 K respectively.



-2749 Time (hours) 0.3 $\tilde{T}\left(K\right)$ (K)-0.3 0 3 4 5 20 22 23 25 Time (hours) Time (hours)

Figure 4: Zero-mean power deviation leads to a nonzero-mean temperature deviation at steady state (plot

Figure 5: Nonzero-mean power deviation used to ensure that the temperature deviation at steady state is zeroshown on the bottom right corner). The values used mean (plot shown on the bottom right corner). The value were: $\Delta P = 0.3 P_{\rm HVAC}^{(b)} = 2917.7$ W, $r_{oa} = 0.5$, and $2t_p = 3600$ seconds. $\Delta P = 0.3 P_{\rm HVAC}^{(b)} = 2917.7$ W, computed from (15). Also $r_{oa} = 0.5$ and $2t_p = 3600$ seconds.

5.1 Nonzero-Mean Power Deviation to Ensure Zero-Mean Temperature Deviation

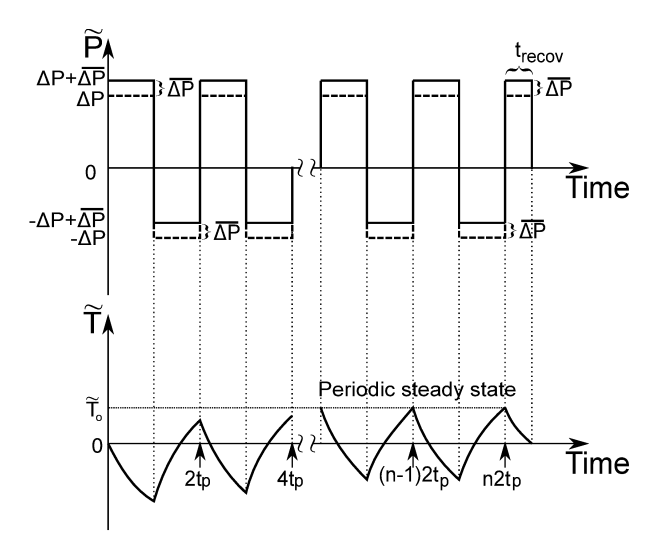
Suppose with a zero-mean square-wave power variation \tilde{P} over the baseline, the mean of \tilde{T} at periodic steady state is positive, meaning the building is on average warmer than the baseline temperature. In order to ensure that the mean of \tilde{T} is 0, an additional constant $\overline{\Delta P} > 0$ will have to be added to \tilde{P} , to provide additional cooling, as shown in Figure 6. Adding a constant $\overline{\Delta P}$ to the power deviation command can be interpreted as the building operating at a new, shifted baseline. Suppose we start with an up/down cycle, there are two possibilities that can occur in principle: $T(n2t_p) > 0$ or $T(n2t_p) < 0$. It follows from Definitions 2 and 3 that the RTE at the end of n cycles of the power deviation command is:

$$\eta_{\rm RT}(n) = \begin{cases} \frac{n(\Delta P - \overline{\Delta P})t_p}{(\Delta P + \overline{\Delta P})(nt_p + t_{recov}(n))} & \text{starting with up/down and } \tilde{T}(n2t_p) > 0, \\ \frac{(\Delta P - \overline{\Delta P})(nt_p + t_{recov}(n))}{n(\Delta P + \overline{\Delta P})t_p} & \text{starting with up/down and } \tilde{T}(n2t_p) < 0, \end{cases}$$

$$(12)$$

where $t_{recov}(n)$ is the additional time needed to bring the temperature to zero at the end of n periods. Figure 6 shows an example of \tilde{P} starting with an up/down cycle and $\tilde{T}(n2t_p)$ being greater than zero. It follows that:

$$\eta_{\rm RT}^{\infty} = \lim_{n \to \infty} \eta_{\rm RT}(n) = \frac{\Delta P - \overline{\Delta P}}{\Delta P + \overline{\Delta P}} < 1.$$
(13)



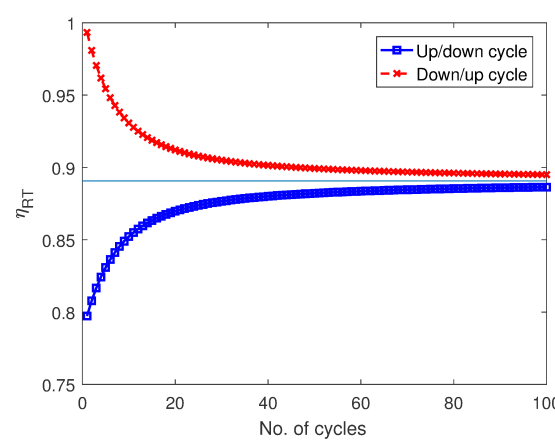


Figure 6: Nonzero-mean power deviation to ensure zero-mean temperature deviation (at steady state). As before, the time t_{recov} is the time needed to bring the temperature deviation to 0 after n periods of the squarewave power deviation. \tilde{T}_o is the maximum value of \tilde{T} after the building reaches steady state.

Figure 7: $\eta_{\rm RT}$ vs n, when the virtual battery tracks a nonzero-mean square-wave power consumption so that the average steady state temperature deviation is zero. $\eta_{\rm RT}^{\infty}=0.8907$ for $\Delta P=0.3P_{\rm HVAC}^{(b)}=2917.7$ W, $r_{oa}=0.5$, and $2t_p=3600$ seconds.

It is to be noted that the same two possibilities can occur when starting with a down/up cycle. However, (13) and the result that $\eta_{RT}^{\infty} < 1$ remain unchanged.

If, on the other hand, the mean temperature deviation is negative when the power deviation command is zero-mean, that would mean the building is colder on average. In order to ensure that the mean of \tilde{T} is 0, an additional constant $\overline{\Delta P}>0$ will have to be subtracted from the original \tilde{P} to provide additional heating. By a similar analysis as above it can be shown that the limiting RTE is:

$$\eta_{\rm RT}^{\infty} = \frac{\Delta P + \overline{\Delta P}}{\Delta P - \overline{\Delta P}} > 1.$$
(14)

To determine the RTE from (13) or (14), we first need to determine $\overline{\Delta P}$. A method for computing $\overline{\Delta P}$ is described in Section 5.2; here we present only the numerical results obtained using that method.

In simulations with parameters described in Section 3.3, we have encountered only the first scenario described above that additional cooling is needed to keep the mean temperature deviation at 0—never additional heating. For $P_{\text{HVAC}}^{(b)} = 9725.6 \text{ W}$, $\Delta P = 0.3 P_{\text{HVAC}}^{(b)}$, $r_{oa} = 0.5$, $2t_p = 3600$ seconds, and all other parameters provided in Section 3.3, the method provided in Section 5.2 yields $\overline{\Delta P} = 168.6 \text{ W}$. Eq. (13) then yields $\eta_{\text{RT}}^{\infty} = 0.8907$. Figure 5 shows the corresponding simulation results, which show that the temperature deviation at steady state is now zero-mean. Figure 7 shows $\eta_{\text{RT}}(n)$ vs. n, determined using (12), where the quantity $t_{recov}(n)$ is estimated from the numerically computed trajectory of $\tilde{T}(t)$. We see from the figure that the numerically estimated values of $\eta_{\text{RT}}(n)$ converges to $\eta_{\text{RT}}^{\infty} = 0.8907$ predicted by (13) (shown as a solid line) as n increases without bound.

5.2 Expressions for $\overline{\Delta P}$ and $ilde{T}_o$

First we present the formulas for $\overline{\Delta P}$ and \tilde{T}_o , where $\overline{\Delta P}$ is the constant that needs to be added to \tilde{P} (zero-mean power-deviation signal) so that the steady-state average of $\tilde{T}=0$, and \tilde{T}_o is the maximum value of the temperature deviation \tilde{T} after the building reaches steady state; see Figure 6. The outline of the procedure we used to derive these formulas is presented in Section 5.2.1.

$$\overline{\Delta P} = \frac{(\mu_1 \mu_4 - 1)(\mu_8 + \mu_{11}) - (\mu_7 + \mu_{10})(\mu_2 \mu_4 + \mu_5)}{-(\mu_1 \mu_4 - 1)(\mu_9 + \mu_{12}) + (\mu_7 + \mu_{10})(\mu_3 \mu_4 + \mu_6)},\tag{15}$$

$$\tilde{T}_o = \frac{-(\mu_8 + \mu_{11}) - (\mu_9 + \mu_{12})\overline{\Delta P}}{(\mu_7 + \mu_{10})},\tag{16}$$

where
$$\mu_1 \triangleq e^{m_1 t_p}$$
, $\mu_2 \triangleq -(n_1 \Delta P + s_1) \Big[\frac{1 - e^{m_1 t_p}}{m_1} \Big]$, $\mu_3 \triangleq -n_1 \Big[\frac{1 - e^{m_1 t_p}}{m_1} \Big]$, $\mu_4 \triangleq e^{m_2 t_p}$,
$$\mu_5 \triangleq (n_2 \Delta P - s_2) \Big[\frac{1 - e^{m_2 t_p}}{m_2} \Big]$$
, $\mu_6 \triangleq -n_2 \Big[\frac{1 - e^{m_2 t_p}}{m_2} \Big]$, $\mu_7 \triangleq \frac{e^{m_1 t_p} - 1}{m_1}$,
$$\mu_8 \triangleq -\frac{(n_1 \Delta P + s_1) t_p}{m_1} + \frac{(n_1 \Delta P + s_1) (e^{m_1 t_p} - 1)}{(m_1)^2}$$
, $\mu_9 \triangleq \frac{n_1 (-m_1 t_p + e^{m_1 t_p} - 1)}{(m_1)^2}$,
$$\mu_{10} \triangleq \frac{\mu_1 (e^{m_2 t_p} - 1)}{m_2}$$
, $\mu_{11} \triangleq \frac{(n_2 \Delta P - s_2) t_p}{m_2} + \frac{(-n_2 \Delta P + s_2) (e^{m_2 t_p} - 1)}{(m_2)^2} + \frac{\mu_2 (e^{m_2 t_p} - 1)}{m_2}$,
$$\mu_{12} \triangleq \frac{n_2 (-m_2 t_p + e^{m_2 t_p} - 1)}{(m_2)^2} + \frac{\mu_3 (e^{m_2 t_p} - 1)}{m_2}$$
,

and the parameters appearing in the formulas of μ 's are given by:

$$m_1 \triangleq -\alpha - \beta \left[\frac{-c}{2d} + \frac{ac - 2db}{2d\sqrt{a^2 + 4d\Delta P}} \right] - \frac{\gamma(-a + \sqrt{a^2 + 4d\Delta P})}{2d}, \quad n_1 \triangleq \frac{-\beta}{\sqrt{a^2 + 4d\Delta P}}, \quad s_1 \triangleq q_1 - n_1 \Delta P,$$

$$(17)$$

$$q_1 \triangleq \frac{-\beta(-a + \sqrt{a^2 + 4d\Delta P})}{2d}, \quad m_2 \triangleq -\alpha - \beta \left[\frac{-c}{2d} + \frac{ac - 2db}{2d\sqrt{a^2 - 4d\Delta P}} \right] - \frac{\gamma(-a + \sqrt{a^2 - 4d\Delta P})}{2d}, \tag{18}$$

$$n_2 \triangleq \frac{-\beta}{\sqrt{a^2 - 4d\Delta P}}, \quad s_2 \triangleq q_2 + n_2 \Delta P, \quad q_2 \triangleq \frac{-\beta(-a + \sqrt{a^2 - 4d\Delta P})}{2d}.$$
 (19)

5.2.1 Derivation of the formulas (15) and (16): We only provide the outline, since the details involve messy algebra that does not offer any insight. Since we are limiting ourselves to times after steady state is reached, we can shift the origin of time so that charging occurs when $t \in [0, t_p]$ and discharging occurs when $t \in [t_p, 2t_p]$. This makes the results valid irrespective of whether the power deviation started with an up/down cycle or down/up cycle, since transients play no role. Let \tilde{T}_o be the maximum value of the temperature deviation \tilde{T} after the building reaches steady state; see Figure 6. Clearly, the maximum temperature will be achieved at the end of a discharging (power-down) half-cycle. That is, $\tilde{T}(0) = \tilde{T}(2t_p) = \tilde{T}_o$. Since our hypothesis is that the mean temperature deviation is zero and the temperature is in (periodic) steady state, we must have the following:

$$\int_0^{2t_p} \tilde{T}(t)dt = 0 \quad \text{and} \quad \tilde{T}(0) = \tilde{T}(2t_p) = \tilde{T}_o. \tag{20}$$

The two equations mentioned above can be solved to determine the two unknowns \tilde{T}_o and $\overline{\Delta P}$. To determine expressions for the left hand side of these equations, we need expressions for the temperature deviation $\tilde{T}(t)$ as a function of the two unknowns. As discussed in Section 3.2, to determine $\tilde{T}(t)$ one has to solve a nonlinear DAE. To determine the required expressions, therefore, we need to perform some simplifications. First, based on numerical evidence, we eliminate one of the roots for (6), which gives:

$$\tilde{m}_a = \frac{-(c\tilde{T} + a) + \sqrt{(c\tilde{T} + a)^2 - 4d(b\tilde{T} - \tilde{P})}}{2d},$$
(21)

so the DAE reduces to the nonlinear ode: $\dot{\tilde{T}}(t) = -\alpha \tilde{T} - \beta \tilde{m}_a - \gamma \tilde{T} \tilde{m}_a$, where \tilde{m}_a is the expression from (21). In order to obtain an analytical solution, we linearize the ODE around two operating points: $(\tilde{T}^*, \tilde{P}^*) = (0, \Delta P)$ and $(\tilde{T}^*, \tilde{P}^*) = (0, -\Delta P)$. The linearized ODEs, respectively, are:

$$\dot{\tilde{T}} = m_1 \tilde{T} + n_1 \tilde{P} + s_1, \tag{22}$$

$$\dot{\tilde{T}} = m_2 \tilde{T} + n_2 \tilde{P} + s_2, \tag{23}$$

where the constants m_i, n_i , and s_i are defined in (17) through (19). The linear ODE (22) is an approximation of the nonlinear differential algebraic system during the charging half period, while the linear ODE (23) is an approximation during the discharging half period. Since linear, time-invariant ODEs have explicit solutions (the so-called variation of constants formula), we can write down the expression for $\tilde{T}(t)$ during $t \in [0, t_p]$, starting with the initial condition $\tilde{T}(0) = \tilde{T}_o$, from (22). Similarly, we can write down the expression for $\tilde{T}(t)$ during $t \in [t_p, 2t_p]$, with the initial condition $\tilde{T}(t_p)$ determined in the previous step, from (23). The variables \tilde{T}_o and $\overline{\Delta P}$ appear as unknown constants in these expressions. Armed with these expressions, we can determine the left sides of the two equations in (20), which are then solved to determine the two unknowns \tilde{T}_o and $\overline{\Delta P}$. This results in the expressions (15) and (16).

5.3 Effect of Various Parameters on η_{RT}^{∞} (in eq. (13))

In this section we examine how $\eta_{\rm RT}^{\infty}$ in (13) depends on various parameters. For every set of parameter values picked, the method described in Section 5.2 was used to compute $\overline{\Delta P}$. The corresponding $\eta_{\rm RT}^{\infty}$ was then computed from (13). Nominal values for the various parameters used in this section are: $r_{oa}=0.5, \Delta P=20\% P_{\rm HVAC}^{(b)}, 2t_p=3600$ seconds, and the values listed in section 3.3.

5.3.1 Building size: We vary the floor area of the building while keeping its height fixed. The baseline air flow rate and the R, C values are assumed to depend on the size of the building in the following manner:

$$m_a^{(b)} = \frac{A_f}{A_f^*} m_a^{(b),*}, \quad C = \frac{A_f}{A_f^*} C^*, \quad R = \frac{A_{ef}^*}{A_{ef}} R^*,$$
 (24)

where A_f is the floor area, A_{ef} is the external surface area of the building (i.e., total surface area minus floor area), and * denotes the nominal values (parameters mentioned in section 3.3). We also increase the exogenous heat gain q_x with increase in building size so that the equilibrium condition in (4) is maintained. We examine two cases. Case (i): the amplitude ΔP of the power deviation is held constant (1945.1 W) as building size changes. Case (ii): ΔP changes with building size according to $\Delta P = 20\% P_{\text{HVAC}}^{(b)}$, where $P_{\text{HVAC}}^{(b)}$ is computed by using $m_a^{(b)}$ from (24) in (3). Figure 8 shows how $\eta_{\text{RT}}^{\infty}$ varies with building size. The figure also shows the product of resistance and capacitance, RC, which is a measure of thermal inertia. We see that for case (i), the RTE increases as building size increases. When building size increases, since ΔP remains the same, the temperature deviation (and therefore its average value) reduces as the building has a higher thermal inertia. Therefore a smaller $\overline{\Delta P}$ is needed, leading to increase in $\eta_{\text{RT}}^{\infty}$. For case (ii), the RTE decreases with building size but with a decaying rate of change. The increase in ΔP with building size leads to a larger temperature deviation. However, the thermal inertia also increases with building size as seen in the previous case, which has an opposing effect on the temperature deviation. The parameter values determine which one of these effects is dominant, and that determines the trend for $\eta_{\text{RT}}^{\infty}$.

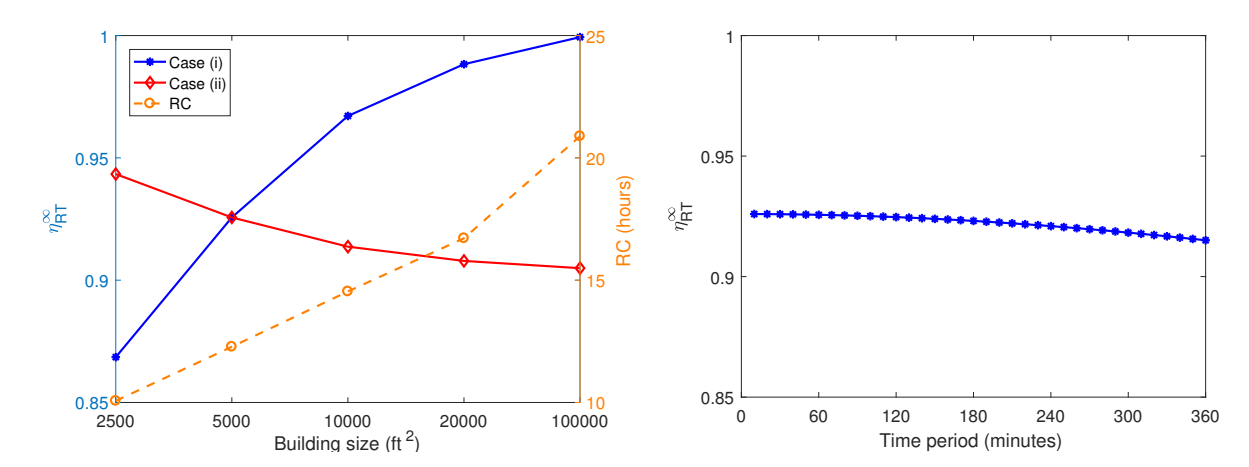


Figure 8: $\eta_{\rm RT}^{\infty}$ (left axis) and RC (right axis) vs. building size; for $r_{oa}=0.5$. Case (i): Same ΔP (1945.1 W) irrespective of building size. Case (ii): ΔP increasing with building size.

Figure 9: $\eta_{\rm RT}^{\infty}$ vs. time period $(2t_p)$; for $r_{oa}=0.5$ and $\Delta P=0.2P_{\rm HVAC}^{(b)}=1945.1$ W.

5.3.2 Time period of the power deviation: Figure 9 shows $\eta_{\rm RT}^{\infty}$ computed for various values of the time period $2t_p$: the RTE decreases slightly as time period increases. To understand this trend, consider the special case of 100% outside air (i.e., $r_{oa}=1$) and a zero-mean square-wave power deviation. Under these conditions the temperature dynamics (the differential algebraic equation discussed in Section 3.2) reduces to two linear time invariant systems (one during charging and the other during discharging) that are asymptotically stable. It can be shown using simple algebra that the steady state temperature deviation during discharging is further away from the baseline temperature than that during charging, and the former is positive, while the latter is negative. The interested readers are referred to the proof of Proposition 1(c) in (Raman & Barooah, 2018) for a detailed discussion regarding the previous statement. This indicates that if t_p is very large, the building is warmer than baseline on average. On the other extreme, if t_p is extremely small, temperature deviation will also be extremely small due to the finite response time of the temperature dynamics. Therefore, as time period increases from 0 to ∞ , the average temperature deviation increases from 0 to a positive constant. Recall that $\overline{\Delta P}$ is added to provide additional cooling to bring the average temperature deviation back to 0. The previous discussion tells us that a larger $\overline{\Delta P}$ is required to do so as time period increases, which leads to a decrease in RTE.

6. CONCLUSION

In this paper, we extended our previous analysis of the RTE of virtual batteries: HVAC systems used to provide a battery-like service to the grid by increasing/decreasing their power demand over a baseline. We showed that imposing an additional constraint, that the mean temperature of the building must remain at its baseline value, can cause asymptotic RTE to be less than 1. Without this constraint the asymptotic RTE is 1. For the range of parameters we examined, the asymptotic RTE is in the range 0.85 - 1, still comparable to that of Li-ion batteries.

Nonlinearity plays a critical role in the analysis. If the models of power and temperature dynamics were both linear, it can be shown using basic linear system theory that a zero-mean deviation of power consumption (from baseline) will lead to a zero-mean deviation of the indoor temperature at steady state. As a result, there is no need for additional cooling (or heating) to keep the temperature deviation zero mean, so the asymptotic RTE is 1.

There are several avenues for further exploration, such as analysis for HVAC systems that provide heating rather than cooling and examination of the role of humidity.

REFERENCES

- Beil, I., Hiskens, I., & Backhaus, S. (2015). Round-trip efficiency of fast demand response in a large commercial air conditioner. *Energy and Buildings*, 97(0), 47 55.
- Cheng, M., Sami, S. S., & Wu, J. (2017). Benefits of using virtual energy storage system for power system frequency response. *Applied Energy*, 194(Supplement C), 376 385.
- Lin, Y. (2014). Control of commercial building HVAC systems for power grid ancillary services (Doctoral dissertation, University of Florida). online.
- Lin, Y., Barooah, P., Meyn, S., & Middelkoop, T. (2015). Experimental evaluation of frequency regulation from commercial building HVAC systems. *IEEE Transactions on Smart Grid*, *6*, 776 783.
- Lin, Y., Mathieu, J. L., Johnson, J. X., Hiskens, I. A., & Backhaus, S. (2017). Explaining inefficiencies in commercial buildings providing power system ancillary services. *Energy and Buildings*, 152, 216 226.
- Luo, X., Wang, J., Dooner, M., & Clarke, J. (2015). Overview of current development in electrical energy storage technologies and the application potential in power system operation. *Applied Energy*, 137, 511 536.
- Makarov, Y., Ma, J., Lu, S., & Nguyen, T. (2008). Assessing the value of regulation resources based on their time response characteristics. *Pacific Northwest National Laboratory*.
- Raman, N., & Barooah, P. (2018, March). On the round-trip efficiency of an HVAC-based virtual battery. *ArXiv e-prints*. (arXiv:1803.02883 [cs.SY])

ACKNOWLEDGMENT

The research reported here has been partially supported by an NSF grant (award no. 1646229) and DOE grant (titled "virtual batteries") under the GMLC program.